

Template-Assisted Solvothermal Synthesis of Five Copper(I)–Thioantimonate(III) Composites: Crystal Structures and Optical and Thermal Properties of $(\text{C}_6\text{N}_2\text{H}_{18})_{0.5}\text{Cu}_2\text{SbS}_3$, $(\text{C}_4\text{N}_3\text{H}_{15})_{0.5}\text{Cu}_2\text{SbS}_3$, $(\text{C}_8\text{N}_4\text{H}_{22})_{0.5}\text{Cu}_2\text{SbS}_3$, $(\text{C}_4\text{N}_3\text{H}_{14})\text{Cu}_3\text{Sb}_2\text{S}_5$, and $(\text{C}_6\text{N}_4\text{H}_{20})_{0.5}\text{Cu}_3\text{Sb}_2\text{S}_5$

V. Spetzler, C. Näther, and W. Bensch*

Institut für Anorganische Chemie, Christian-Albrechts-Universität Kiel, Olshausenstrasse 40, D-24098 Kiel, Germany

Received February 4, 2005

The novel copper(I)–thioantimonates(III) $(\text{C}_6\text{N}_2\text{H}_{18})_{0.5}\text{Cu}_2\text{SbS}_3$ (**I**) ($\text{C}_6\text{N}_2\text{H}_{16}$ = 1,6-diaminohexane), $(\text{C}_4\text{N}_3\text{H}_{15})_{0.5}\text{Cu}_2\text{SbS}_3$ (**II**) ($\text{C}_4\text{N}_3\text{H}_{13}$ = diethylenetriamine), $(\text{C}_8\text{N}_4\text{H}_{22})_{0.5}\text{Cu}_2\text{SbS}_3$ (**III**) ($\text{C}_8\text{N}_4\text{H}_{20}$ = 1,4-bis(2-aminoethyl)piperazine), $(\text{C}_4\text{N}_3\text{H}_{14})\text{Cu}_3\text{Sb}_2\text{S}_5$ (**IV**) ($\text{C}_4\text{N}_3\text{H}_{13}$ = diethylenetriamine), and $(\text{C}_6\text{N}_4\text{H}_{20})_{0.5}\text{Cu}_3\text{Sb}_2\text{S}_5$ (**V**) ($\text{C}_6\text{N}_4\text{H}_{18}$ = triethylenetetramine) were synthesized under solvothermal conditions reacting Sb, Cu, and S with the amines. The compounds **I–III** belong to the RCu_2SbS_3 structure family (R = amine) and are built up of trigonal SbS_3 pyramids and two CuS_3 moieties forming 6-membered (6 MR) and 10-membered (10 MR) rings. The rings are condensed yielding single layers which are joined into $[\text{Cu}_2\text{SbS}_3]^-$ double layers via Cu–S bonds. The organic ions are located between the anionic layers, and the shortest interlayer distances are 7.8 Å (**I**), 7.4 Å (**II**), and 8.8 Å (**III**). The structure of the novel inorganic–organic hybrid compound **IV** contains one SbS_3 group, one SbS_4 unit, two CuS_3 triangles, and one CuS_4 tetrahedron. These units are joined into four-membered (4 MR) and six-membered rings (6 MR) forming a hitherto unknown strong undulated layered $(\text{Cu}_3\text{Sb}_2\text{S}_5)^-$ anion. Anions and cations are arranged in a sandwichlike manner with an interlayer distance of 6.184 Å. The new composite **V** contains an anion with the same chemical composition as compound **IV**, but the structure exhibits a unique and different network topology which is constructed by two SbS_3 pyramids, two CuS_3 triangles, and one CuS_4 tetrahedron. These units are joined into 6 MR which may be described as an inorganic graphene-like layer or as a 6^3 net. Two such layers are connected via Cu–S bonds into the final double layer. The interlayer distance amounts to 6.44 Å. All compounds decompose in a more or less complex manner when heated in an inert atmosphere.

Introduction

During the past decades a large number of thioantimonates(III) were synthesized under solvothermal conditions,^{1–17}

and in several compounds a transition metal ion (TM^{n+}) is part of the SbS_x network.^{18–33} The latter compounds exhibit

* Author to whom correspondence should be addressed. E-mail: wbensch@ac.uni-kiel.de.

- (1) Dittmar, G.; Schäfer, H. Z. *Anorg. Allg. Chem.* **1977**, *437*, 183–187.
- (2) Graf, H. A.; Schäfer, H. Z. *Anorg. Allg. Chem.* **1975**, *414*, 220–230.
- (3) Dittmar, G.; Schäfer, H. Z. *Anorg. Allg. Chem.* **1978**, *441*, 93–97.
- (4) Eisenmann, B.; Schäfer, H. Z. *Naturforsch.* **1979**, *34b*, 383–385.
- (5) Cordier, G.; Schäfer, H.; Schwidetzky, C. Z. *Naturforsch.* **1984**, *39b*, 131–134.
- (6) Volk, K.; Bickert, P.; Kolmer, R.; Schäfer, H. Z. *Naturforsch.* **1979**, *34b*, 380–382.
- (7) Wang, X.; Liebau, F. J. *Solid State Chem.* **1994**, *111*, 385–389.
- (8) Wang, X. *Eur. J. Solid State Inorg. Chem.* **1995**, *32*, 303–312.
- (9) Schur, M.; Bensch, W. Z. *Anorg. Allg. Chem.* **1998**, *624*, 310–314.

- (10) Rijnberk, H.; Näther, C.; Schur, M.; Jess, I.; Bensch, W. *Acta Crystallogr.* **1998**, *C54*, 920–923.
- (11) Schimek, G. L.; Kolis, J. W. *Inorg. Chem.* **1997**, *36*, 1689–1693.
- (12) Volk, K.; Schäfer, H. Z. *Naturforsch.* **1979**, *34b*, 172–175.
- (13) Parise, J. B. *Science* **1991**, *251*, 293–294.
- (14) Parise, J. B.; Ko, Y. *Chem. Mater.* **1992**, *4*, 1446–1450.
- (15) Wang, X.; Jacobson, A. J.; Liebau, F. J. *Solid State Chem.* **1998**, *140*, 387–395.
- (16) Wang, X.; Liu, L.; Jacobson, A. J. *Solid State Chem.* **2000**, *155*, 409–416.
- (17) Ko, Y.; Tan, K.; Parise, J. B.; Darovsky, A. *Chem. Mater.* **1996**, *8*, 493–496.
- (18) Stephan, H.-O.; Kanatzidis, M. G. *Inorg. Chem.* **1997**, *36*, 6050–6057.
- (19) Bensch, W.; Schur, M. Z. *Naturforsch.* **1997**, *52b*, 405–409.

new network topologies and show different physical properties which are significantly different from the TM^{n+} free materials. A series of isostructural manganese thioantimonates(III) $\text{Mn}_2\text{Sb}_2\text{S}_5 \cdot \text{L}$ (L = methylamine, ethylamine, 1,3-diaminopropane, *N*-methyl-1,3-diaminopropane, diethylenetriamine) were synthesized and characterized in our group with Mn^{2+} being a part of the thioantimonate(III) network.^{25,31,32} Further examples are $[\text{Co}(\text{C}_6\text{H}_{18}\text{N}_4)]_2\text{Sb}_4\text{S}_8$ and $[\text{Co}(\text{C}_6\text{H}_{18}\text{N}_4)]_2\text{Sb}_2\text{S}_5$ with the anions bridging the $[\text{TML}_n]^{x+}$ (L = ligand) complexes.^{26,33} Copper–chalcogeno–antimonates(III) were reported in the past containing protonated or nonprotonated amines.^{27–30} In $\text{Cu}_2\text{SbS}_3 \cdot 0.5\text{en}$ (en = ethylenediamine),²⁷ $\text{Cu}_2\text{SbSe}_3 \cdot 0.5\text{en}$, and $\text{Cu}_2\text{SbSe}_3 \cdot \text{en}$ the existence of mixed-valent Cu^{II} and nonprotonated ethylenediamine was postulated.²⁸ In $(\text{C}_4\text{H}_{12}\text{N}_2)_{0.5}\text{CuSb}_6\text{S}_{10}$,²⁹ $(\text{enH}_2)_{0.5}\text{Cu}_2\text{SbS}_3$, (1,3-DAPH₂)_{0.5} Cu_2SbS_3 (1,3-DAP = 1,3-diaminopropane), and (1,4-DABH₂)_{0.5} Cu_2SbS_3 (1,4-DAB = 1,4-diaminobutane) $\text{Cu}(\text{I})$ fully protonated amines are present.³⁰ In these compounds the anionic layers are separated by the amines. The interlayer separations depend on the size and packing of the different amines. Most of these inorganic–organic hybrid compounds show layered structures with a sandwichlike arrangement, which may be regarded as nanostructures.³⁴

In our continuing work we prepared new copper thioantimonates under solvothermal conditions applying different amines as solvents and as structure-directing agents. In this contribution the syntheses, crystal structures, thermal stability, and optical spectroscopy data for the compounds $(\text{C}_6\text{N}_2\text{H}_{18})_{0.5}\text{Cu}_2\text{SbS}_3$ (**I**), $(\text{C}_4\text{N}_3\text{H}_{15})_{0.5}\text{Cu}_2\text{SbS}_3$ (**II**), $(\text{C}_8\text{N}_4\text{H}_{22})_{0.5}\text{Cu}_2\text{SbS}_3$ (**III**), $(\text{C}_4\text{N}_3\text{H}_{14})\text{Cu}_3\text{Sb}_2\text{S}_5$ (**IV**), and $(\text{C}_6\text{N}_4\text{H}_{20})_{0.5}\text{Cu}_3\text{Sb}_2\text{S}_5$ (**V**) are presented. In addition, the structural and spectroscopic properties of compounds **I–III** are compared with those of the previously reported compounds $(\text{enH}_2)_{0.5}\text{Cu}_2\text{SbS}_3$ (**I**), (1,3-DAPH₂)_{0.5} Cu_2SbS_3 (1,3-DAP = 1,3-

diaminopropane) (**2**), and (1,4-DABH₂)_{0.5} Cu_2SbS_3 (**3**) (1,4-DAB = 1,4-diaminobutane).³⁰

Experimental Details

Syntheses. The five compounds $(\text{C}_6\text{N}_2\text{H}_{18})_{0.5}\text{Cu}_2\text{SbS}_3$ (**I**), $(\text{C}_4\text{N}_3\text{H}_{15})_{0.5}\text{Cu}_2\text{SbS}_3$ (**II**), $(\text{C}_8\text{N}_4\text{H}_{22})_{0.5}\text{Cu}_2\text{SbS}_3$ (**III**), $(\text{C}_4\text{N}_3\text{H}_{14})\text{Cu}_3\text{Sb}_2\text{S}_5$ (**IV**), and $(\text{C}_6\text{N}_4\text{H}_{20})_{0.5}\text{Cu}_3\text{Sb}_2\text{S}_5$ (**V**) were prepared under solvothermal conditions in Teflon-lined steel autoclaves. For **I–IV** a mixture of Cu (2 mmol), Sb (2 mmol), S (5 mmol), and 5 mL of 1,6-diaminohexane (**I**), 5 mL of diethylenetriamine (**II** and **IV**), and 5 mL of triethylenetetramine (70%) (**III**), respectively, was heated at 140 °C for 7 days followed by cooling to room temperature. For the synthesis of compound **V** the same mixture of elements was heated with 4 mL of triethylenetetramine (97%) at 140 °C for 9 days. The products were filtered off and washed with deionized water and dry acetone. Crystals were obtained with a yield of about 60% (**I**, **II**) and 30% (**III**) based on Cu. Compound **II** occurred always together with **IV** (<30%). The yield of compound **V** was between 50 and 60% based on Cu. In the product of **III** red needles were identified as $(\text{C}_6\text{N}_4\text{H}_{20})\text{Sb}_4\text{S}_7$ ($\text{C}_6\text{N}_4\text{H}_{20}$ = double protonated tris(2-aminoethyl)amine). Anal. Found (%) for **I**: C, 8.2; H, 2.04; N, 3.2. Calcd: C, 7.8; H, 1.9; N, 3.0. Found for **II**: C, 5.2; H, 1.4; N, 4.3. Calcd: C, 5.5; H, 1.5; N, 4.6. Found for **III**: C, 3.9; H, 0.91; N, 2.9. Calcd: C, 4.2; H, 1.1; N, 3.2. Found for **IV**: C, 6.6; H, 1.9; N, 5.7. Calcd: C, 6.9; H, 2.1; N, 5.9. Found for **V**: C, 4.8; H, 1.2; N, 3.6. Calcd: C, 4.9; H, 1.3; N, 4.0.

X-ray Scattering Studies. The X-ray intensity data were collected at 293 K using a NONIUS CAD4 for **I** and a STOE AED 4 diffractometer for **II–V** with graphite-monochromated Mo $\text{K}\alpha$ radiation ($\lambda = 0.71073 \text{ \AA}$). The raw intensities were treated in the normal way by applying a Lorentz–polarization correction. The data were also corrected for absorption effects. The structures were solved using SHELXS-97.³⁵ Crystal structure refinements were done against F^2 with SHELXL-97.³⁶ All non-hydrogen atoms were refined with anisotropic displacement parameters. The hydrogen atoms were positioned with idealized geometry and refined with fixed isotropic displacement parameters using a riding model. The amine molecules in **I** and **II** are partially disordered around a center of inversion and were refined using a split model. The site occupation factors were refined to 50:50 (C3:C3') for **I** and to 60:40 (C1:C1', C2:C2', N1:N1', and N2:N2') for **II**. In compounds **IV** and **V** the strong disorder of the amines prevented a successful refinement. Hence, the SQUEEZE option in the program package Platon was used to correct the structure factors.³⁷ Details of the data collections and refinement results are summarized in Table 1. Bond lengths and angles for all compounds are listed in Tables 2, 4, and 5.

Spectroscopy. The Raman spectra were measured from 100 to 500 cm^{-1} with a Bruker IFS 66 Fourier transform Raman spectrometer (wavelength, 514.5 nm; $T = 20 \text{ K}$).

Thermoanalytical Investigations. Thermogravimetry analyses were performed using a Netzsch STA 429 DTA-TG device. The samples were heated in Al_2O_3 crucibles at a rate of 4 $\text{K}\cdot\text{min}^{-1}$ to 400 °C under a flow of argon of 100 mL min^{-1} .

Results and Discussion

The three compounds $(\text{C}_6\text{N}_2\text{H}_{18})_{0.5}\text{Cu}_2\text{SbS}_3$ (**I**) $(\text{C}_4\text{N}_3\text{H}_{15})_{0.5}\text{Cu}_2\text{SbS}_3$ (**II**), and $(\text{C}_8\text{N}_4\text{H}_{22})_{0.5}\text{Cu}_2\text{SbS}_3$ (**III**) crystallize in

- (20) Kiebach, R.; Näther, C.; Bensch, W. *Z. Anorg. Allg. Chem.* **2002**, *628*, 2176–2181.
 (21) Stähler, R.; Bensch, W. *Eur. J. Inorg. Chem.* **2001**, 3073–3078.
 (22) Stähler, R.; Näther, C.; Bensch, W. *Acta Crystallogr.* **2001**, *C57*, 26–27.
 (23) Stähler, R.; Bensch, W. *Z. Anorg. Allg. Chem.* **2002**, *628*, 1657–1662.
 (24) Schäfer, M.; Näther, N.; Bensch, W. *Solid State Sci.* **2003**, *5*, 1135–1139.
 (25) Engelke, L.; Stähler, R.; Schur, M.; Näther, C.; Bensch, W.; Pöttgen, R.; Möller, M. H. *Z. Naturforsch.* **2004**, *59b*, 869–876.
 (26) Schäfer, M.; Stähler, R.; Kiebach, W.-R.; Näther, C.; Bensch, W. *Z. Anorg. Allg. Chem.* **2004**, *630*, 1816–1822.
 (27) Powell, A. V.; Boissiere, S.; Chippendale, A. M. *J. Chem. Soc., Dalton Trans.* **2000**, 4192–4195.
 (28) Chen, Zh.; Dillks, R. E.; Wang, R.-J.; Lu, J. Y.; Li, J. *Chem. Mater.* **1998**, *10*, 3184–3188.
 (29) Powell, A. V.; Paniagua, R.; Vaqueiro, P.; Chippendale, A. M. *Chem. Mater.* **2002**, *14*, 1220–1224.
 (30) Spetzler, V.; Rijnberk, H.; Näther, C.; Bensch, W. *Z. Anorg. Allg. Chem.* **2004**, *630*, 142–148.
 (31) Bensch, W.; Schur, M. *Eur. J. Solid State Inorg. Chem.* **1996**, *33*, 1149–1160.
 (32) Schur, M.; Näther, C.; Bensch, W. *Z. Naturforsch.* **2001**, *56b*, 79–84.
 (33) Stähler, R.; Bensch, W. *J. Chem. Soc., Dalton Trans.* **2001**, 2518–2522.
 (34) Lurf, A. In *Handbook of Nanostructured Materials and Nanotechnology*; Nalwa, H. S., Ed.; Academic Press: New York, 2000; Vol. 5. Lurf, A. In *Intercalated Layered Materials*; Lévy, F. A., Ed.; D. Reidel Publishing: Dordrecht, Boston, London, 1979.

- (35) Sheldrick, G. M. *SHELXS-97, Program for Crystal Structure Solution*; University of Göttingen: Göttingen, Germany, 1997.
 (36) Sheldrick, G. M. *SHELXL-97, Program for the Refinement of Crystal Structures*; University of Göttingen: Göttingen, Germany, 1997.
 (37) Spek, A. L. *Platon for Windows*; Utrecht University: Utrecht, The Netherlands, 2000.

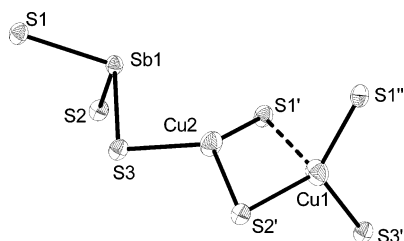
Table 1. Selected Crystallographic Data and Refinement Results for $(C_6N_2H_{18})_{0.5}Cu_2SbS_3$ (**I**), $(C_4N_3H_{15})_{0.5}Cu_2SbS_3$ (**II**), $(C_8N_4H_{22})_{0.5}Cu_2SbS_3$ (**III**), $(C_4N_3H_{14})Cu_3Sb_2S_5$ (**IV**), and $(C_6N_4H_{20})_{0.5}Cu_3Sb_2S_5$ (**V**)

param	I	II	III	IV	V
$a/\text{\AA}$	6.1401(12)	6.1962(4)	6.1594(12)	23.6408(16)	6.3188(8)
$b/\text{\AA}$	24.7704(5)	22.4696(18)	27.4803(6)	20.4108(15)	9.9523(13)
$c/\text{\AA}$	6.5545(13)	6.5461(4)	6.5491(13)	6.4599(7)	11.3630(13)
α/deg					103.376(14)
β/deg	112.530(10)	112.47(6)	112.24(3)	100.153(7)	91.420(14)
γ/deg					108.340(14)
$V/\text{\AA}^3$	919.0 (2)	842.20(10)	1026.01(4)	3068.3(2)	656.19(14)
$d_{\text{calc}}/\text{g cm}^{-3}$	2.921	3.136	2.791		
cryst system	monoclinic	monoclinic	monoclinic	monoclinic	triclinic
space group	$P2_1/n$	$P2_1/n$	$P2_1/n$	$C2/c$	$P\bar{1}$
$2\theta/\text{deg}$	3–60	4–56	3–52	5–56	4–60
hkl range	$0 \leq h \leq 8$ $-32 \leq k \leq 32$ $-8 \leq l \leq 7$	$-8 \leq h \leq 8$ $-29 \leq k \leq 29$ $-8 \leq l \leq 8$	$-7 \leq h \leq 7$ $-33 \leq k \leq 33$ $-8 \leq l \leq 8$	$-31 \leq h \leq 31$ $-26 \leq k \leq 26$ $-8 \leq l \leq 8$	$-7 \leq h \leq 7$ $-11 \leq k \leq 10$ $-13 \leq l \leq 12$
no. collcd reflcns	4745	7739	7806	14 656	3714
no. unique reflcns	2215	1954	1957	3587	2173
reflcn $F_o > 4\sigma(F_o)$	2062	1691	1753	2624	1485
params	92	108	117	92	91
R1 ($F_o > 4\sigma(F_o)$)	0.0161	0.0299	0.0280	0.0407	0.0639
wR2 ($F_o > 4\sigma(F_o)$)	0.0395	0.0736	0.0689	0.0944	0.1623
R1 (all reflcns)	0.0190	0.0371	0.0343	0.0609	0.0863
wR2 (all reflcns)	0.0401	0.0766	0.0713	0.1002	0.1691
GOF	1.129	1.036	1.032	0.925	0.961
$\delta(F)/e \text{\AA}^{-3}$	0.532/–0.529	0.832/–1.839	0.73/–1.44	1.063/–1.272	2.448/–2.630

Table 2. Ranges of Interatomic Distances (\AA) and Angles (deg) for $(C_6N_2H_{18})_{0.5}Cu_2SbS_3$ (**I**), $(C_4N_3H_{15})_{0.5}Cu_2SbS_3$ (**II**), and $(C_8N_4H_{22})_{0.5}Cu_2SbS_3$ (**III**) with Estimated Standard Deviations in Parentheses

	I	II	III
Cu(1)–S	2.271(1)–2.327(1)	2.280(1)–2.338(1)	2.277(1)–2.332(1)
Cu(2)–S	2.316(1)–2.367(1)	2.315(1)–2.361(1)	2.313(1)–2.358(1)
Sb–S	2.422(1)–2.450(1)	2.435(1)–2.459(1)	2.427(1)–2.454(1)
Cu–Sb	2.726(1)–3.075(1)	2.737(1)–3.094(1)	2.726(1)–3.086(1)
Cu(1)–S(1a)	2.954(2)	2.989(1)	2.977(1)
Cu(2)–Cu(1)	2.633(1)	2.646(1)	2.635(1)
S–Cu(1)–S	113.46(3)–122.32(2)	113.65(4)–122.19(5)	114.02(5)–121.25(5)
S–Cu(2)–S	105.33(2)–122.88(3)	105.83(5)–123.31(4)	105.41(5)–123.65(5)
S–Sb–S	98.08(2)–100.77(2)	98.24(4)–99.70(4)	98.69(4)–99.79(4)

the monoclinic space group $P2_1/n$ with four formula units in the unit cell, and they are isostructural with $(enH_2)_{0.5}Cu_2SbS_3$ (**1**), $(1,3\text{-DAPH}_2)_{0.5}Cu_2SbS_3$ (**1,3-DAP** = 1,3-diaminopropane) (**2**), and $(1,4\text{-DABH}_2)_{0.5}Cu_2SbS_3$ (**3**) (1,4-DAB = 1,4-diaminobutane).³⁰ Hence, the structure is only briefly discussed. In many thioantimonates(III) the Sb–S distances scatter from about 2.4 to 3.8 \AA and a consistent assignment of the dimensionality depends on the cutoff chosen. In the present contribution the description of the structures is restricted to a cutoff for the Sb–S distances of about 3.1 \AA . The primary building units (PBUs) in **I–III** are one trigonal SbS_3 pyramid and two CuS_3 moieties (Figure 1). The Sb–S bond lengths and S–Sb–S angles (see Table 2) are in the range found in many other thioantimonates(III).^{18–33} The Sb atom has a Cu(2) atom as the next-nearest neighbor (Table

**Figure 1.** Environment of Sb1, Cu1, and Cu2 in the crystal structure of compound **I**. (Dotted line indicates a long bond.) Displacement ellipsoids are drawn at the 60% probability level.

2), and with this atom a distorted $SbS_3Cu(2)$ tetrahedron is formed. The Cu(1) atom is located at the apex of a flat trigonal pyramid with 3 S atoms forming the basis of the pyramid (Figure 1) and is 0.2589 \AA (**II**), 0.2447 \AA ; **III**, 0.2523 \AA) above this plane. The Cu(1)–S bond lengths and S–Cu(1)–S angles (Table 2) are similar to the values observed for the other three isostructural compounds.³⁰ In **I–III** the Cu(1) atoms have an additional relatively long contact expanding the pyramid into a strongly distorted $Cu(1)S_4$ tetrahedron (Table 2, Figure 1). If the Sb atom is considered as another neighbor, a distorted rectangular $Cu(1)SbS_4$ pyramid may be identified (Figure 1). The Cu(2) atom is also in a trigonal environment of three S atoms and is situated 0.5405 \AA (**I**) above the plane formed by the S atoms (0.5220 \AA (**II**), 0.5281 \AA (**III**)). The Cu(2)–S distances and the S–Cu(2)–S angles are in close agreement with data published for the compounds (**1–3**).³⁰ Cu(2) has an Sb and Cu(1) as next neighbors with a Cu–Cu distance which is slightly longer than in Cu metal (2.556 \AA) or in other sulfides and selenides for which a $d^{10}\text{–}d^{10}$ interaction was discussed^{38,39} (see Figure 1 and Table 2). The Cu–Cu distances in oligomers and polymers are in some compounds about 0.2 \AA shorter than in metallic Cu which was explained

(38) Jansen, M. *Angew. Chem.* **1987**, *99*, 1136–1149.(39) Merz, K. M.; Hoffmann, R., Jr. *Inorg. Chem.* **1988**, *27*, 2120–2127.

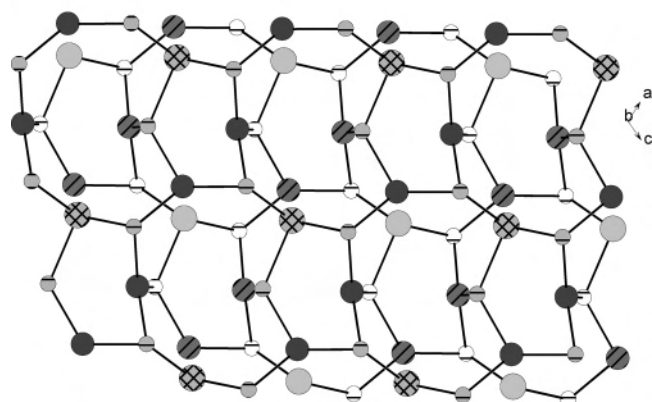
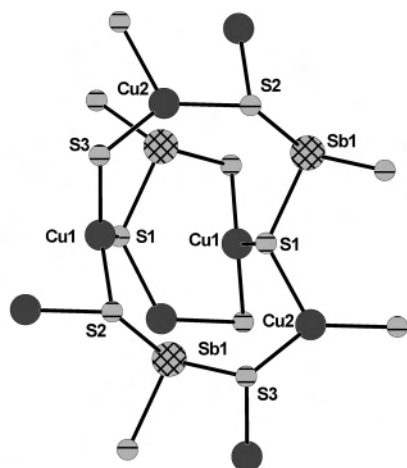


Figure 2. 10-membered ring 10 MR and the 6-membered ring 6 MR below the 10 MR in compounds **I–III** (top) and the interconnection of 10 MR and 6 MR into the final $[\text{CuSbS}_3]^-$ layer (bottom). Note that the Sb and S atoms of neighbored layers have a different color/shading.

by a mixing of 4s and 4p orbitals into 3d orbitals, converting repulsive $d^{10}-d^{10}$ interactions into partial bonding.³⁹ A comparison of the geometrical parameters of the three compounds reveals only small differences (Table 2).

The connection of SbS_3 , $\text{Cu}(1)\text{S}_3$, and $\text{Cu}(2)\text{S}_3$ units yields 6-membered (6 MR) Cu_2SbS_3 rings and 10-membered rings (10 MR) $\text{Cu}_3\text{Sb}_2\text{S}_5$ (Figure 2, top). Every 10 MR is condensed to four 10 MR and four 6 MR to form a single layer within the (010) plane (Figure 2, bottom). Two such single layers are connected into the final $[\text{CuSbS}_3]^-$ layered anion, and due to the 2_1 screw axis and the n glide plane the 6 MR are above and below the 10 MR (Figure 2, bottom). In the description of the interconnection of the SbS_3 pyramids and the CuS_3 units $\text{Cu}-\text{Cu}$ and $\text{Cu}-\text{Sb}$ contacts were neglected. The Sb atom has four next-nearest S neighbors at distances in the range for the sum of the van der Waals radii of Sb and S.

The amines are located between successive anionic layers yielding a sandwichlike arrangement (Figure 3). Similar to the previously reported isostructural compounds (**1–3**) the NH_3 groups are oriented toward the $[\text{CuSbS}_3]^-$ layers achieving optimal $\text{S}\cdots\text{H}$ interactions (Table 3).

The interlayer distances are determined by the lengths of the amine molecules and their relative orientation with respect to the anionic layers. For $\text{Cu}_2\text{SbS}_3 \cdot 0.5\text{en}$ the separa-

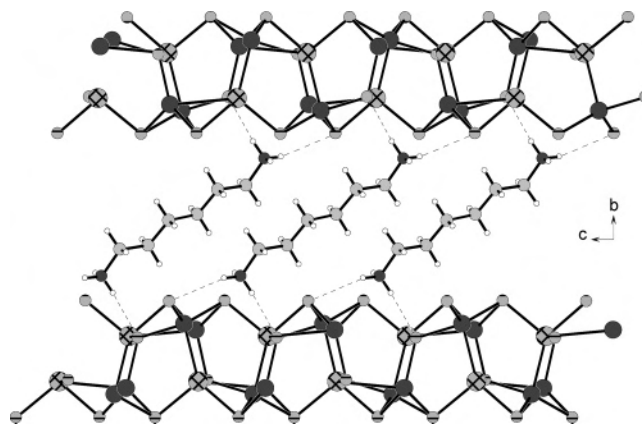


Figure 3. Crystal structure of compound **I** with view along the a -axis. (Intermolecular $\text{S}-\text{H}$ bonds are indicated as dotted lines.)

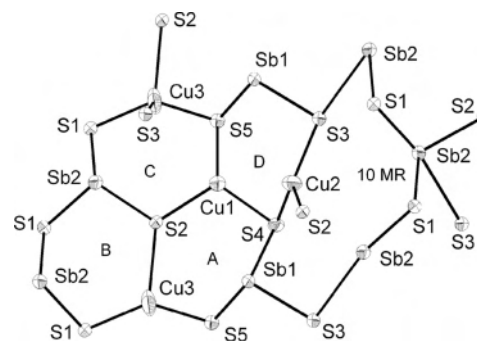


Figure 4. Crystal structure of compound **IV** with labeling showing the different rings. Displacement ellipsoids are drawn on the 50% probability level. The letters identify the different heterorings discussed in the text.

Table 3. $\text{N}\cdots\text{S}$ Distances (\AA) in $(\text{C}_6\text{N}_2\text{H}_{18})_{0.5}\text{Cu}_2\text{SbS}_3$ (**I**), $(\text{C}_4\text{N}_3\text{H}_{15})_{0.5}\text{Cu}_2\text{SbS}_3$ (**II**), and $(\text{C}_8\text{N}_4\text{H}_{22})_{0.5}\text{Cu}_2\text{SbS}_3$ (**III**)

	I	II	III
	3.161 (S1)	3.158 (S1)	3.178 (S1)
	3.286 (S2)	3.329 (S2)	3.292 (S2)
	3.301 (S3)	3.401 (S3)	3.337 (S3)

tion amounts to 5 \AA .²⁷ For compounds (**1–3**) the values are 4.426(4), 5.986(1), and 5.931(1) \AA , respectively.³⁰ In **I–III** the interlayer distances are 7.441(1), 7.446(2), and 8.842(5) \AA . The increase of the interlayer spacing going from **I** to **III** is accompanied by a longer crystallographic b axis. The thickness of inorganic host lattices is often in the range from 3 to 10 \AA , and the layer separations caused by intercalated species can vary from 3 to 50 \AA . For instance, an interlayer distance of 56.1 \AA was reported for $(\text{octadecylamine})_x\text{TaS}_2$. Such compounds belong to the so-called “nanostructured systems”,³⁴ and consequently, compounds **I–III** belong also to this type of materials.

An interesting observation is that triethylenetetramine (TETN) (**III**) cyclizes under the solvothermal conditions forming the protonated 1,4-bis(2-ammoniomethyl)piperazine cation. It is known that TETN decomposes under special synthetic conditions to form ethylenediamine and cyclized amines, including piperazine (pip).⁴⁰ Parise et al. reported the synthesis of $\text{Sb}_4\text{S}_7 \cdot \text{N}_2\text{C}_4\text{H}_8$ with a piperazinium cation formed in-situ by applying TETN as solvent.⁴⁰ It is known that under pyrolytic conditions amines cyclize and form

(40) Parise, J. B. *Chem. Mater.* **1992**, *4*, 1446–1450.

Table 4. Ranges of Interatomic Distances (Å) and Angles (deg) for (C₄N₃H₁₄)Cu₃Sb₂S₅ (**IV**) with Estimated Standard Deviations in Parentheses

Sb(1)–S	2.416(2)–2.450(2)
Sb(1)–Cu	2.927(1)–3.016(1)
Sb(2)–S	2.434(2)–3.037(1)
Cu(1)–S	2.290(2)–2.320(2)
Cu(2)–S	2.278(2)–2.336(2)
Cu(3)–S	2.290(2)–2.595(2)
Cu–Cu	2.622(1)–2.857(2)
S–Sb(1)–S	99.35(6)–104.11(6)
S–Sb(2)–S	87.73(5)–168.12(5)
S–Cu(1)–S	112.66(7)–120.84(7)
S–Cu(2)–S	113.92(8)–121.88(8)
S–Cu(3)–S	95.83(7)–124.39(8)

amines such as 1,4-bis(2-aminoethyl)piperazine.⁴⁰ We note that our TETN (70%) solution was a mixture with about 30% tris(2-aminoethyl)amine (C₆N₄H₁₈), which can be responsible for the ring formation too.

The new compound (C₄N₃H₁₄)Cu₃Sb₂S₅ (**IV**) crystallizes in the monoclinic space group *C2/c* with two unique Sb atoms, three independent Cu atoms, and 5 unique S atoms. Sb(1) is in a trigonal pyramidal environment of 3 S atoms, and Sb(2) is coordinated by four S atoms with two long and two short bonds (Figure 4, Table 4). The Sb(2)S₄ moiety may be described as trigonal bipyramidal considering the electron lone pair as a coordination site. In such SbS₄ units the long Sb–S bonds are in trans position. Up to the sum of the van der Waals radii of Sb and S of about 3.80 Å Sb(1) has two additional S atoms and Sb(2) one S atom as neighbors. Cu(1) is surrounded by three S atoms and is situated 0.304 Å above the S₃ plane forming a trigonal Cu(1)S₃ moiety (Figure 4, Table 4). Two additional contacts to Sb(1) and Cu(2) are observed (Table 4), and the resulting coordination polyhedron may be described as a distorted rectangular pyramid like in the other compounds (see above³⁰). Cu(2) is also coordinated by three S atoms (Figure 4), but the Cu(2)S₃ group is more flat than Cu(1)S₃ with Cu(2) being 0.1858 Å above the plane formed by the three S atoms. There are additional contacts to Cu(1), Cu(3), and Sb(1) with a Cu(2)–Cu(3) distance which is shorter than the Cu–Cu separations in compounds **I–III** (compare Tables 2 and 4) but slightly longer than in Cu metal (2.556 Å).^{38,39} Cu(3) has bonds to 4 S atoms within an distorted tetrahedron (Figure 4).

The PBUs are joined to form different puckered heterorings: Sb(1)Cu(1)Cu(3)S₃ (6 MR A), Sb(2)₂Cu(3)S₃ (6 MR B), Sb(2)Cu(1)Cu(3)S₃ (6 MR C), Sb(1)Cu(1)Cu(2)S₃ (6 MR D), (Sb(1)Sb(2)₃Cu(2)S₅ (10 MR) (Figure 5, top). These SBUs are then condensed to form a single layer. Along [010] the sequence of the different rings is ⋯A–B–C–D–10 MR–10 MR–A–B–C–D⋯ (Figure 5, top). The 10 MR are condensed along [001], and the 6 MR show the sequence ⋯A–D–A–D⋯ and ⋯B–C–B–C⋯ (Figure 5, top). (Figure 5, top). Further interconnection of the single layer proceeds via an A ring containing the Cu(3)S₄ tetrahedron and which is located above (below) each D ring. The Cu(3) atom of the A ring is bound to S(3) of the D ring, and Cu(2) of the D ring has a bond to S(2) of the A ring. Furthermore, the atoms of the A (D) ring above (below) have bonds to

atoms of the 10 MR yielding a 6 MR type E ring (Sb(1)Sb(2)Cu(2)S₃) and two 4 MR (Sb(2)Cu(3)S₂, Cu(2)Cu(3)S₂). Interestingly, the Sb(2) atom of the 6 MR type C is involved in a 6 MR of type E, which is below (above) the 6 MR C. The interconnection mode generates a double-layer thick central part of the undulated anion (Figure 5, bottom). The layers within the (001) plane are separated by the organic amine cations, and a sandwichlike arrangement of anions and cations is observed. The shortest interlayer S–S distance is 6.184 Å (measured from coordinate to coordinate).

The novel compound (C₆N₄H₂₀)_{0.5}Cu₃Sb₂S₅ (**V**) crystallizes in the triclinic space group *P1̄* with two formula units in the unit cell. All atoms are on general positions. Two trigonal SbS₃ pyramids, two CuS₃ moieties, and one CuS₄ tetrahedron are the PBUs (Figure 6). The Sb–S bond lengths and angles are in the normal range (Table 5). Each Sb atom has one S atom at a longer distance of about 3.5 Å. Cu(1) is tetrahedrally coordinated by 4 S atoms, and the distortion of the Cu(1)S₄ tetrahedron is less pronounced than that of the Cu(3)S₄ tetrahedron in **IV** (Table 5). The distance Cu(1)–Cu(1a) of 2.715(5) Å is longer than in the compounds presented above. The two other Cu atoms are trigonally coordinated by three S atoms with Cu–S distances and angles in the range observed in the other compounds (Table 5). The S–Cu–S angles indicate a different degree of distortion, which is also evident by the position of the Cu atoms above the planes formed by the three S atoms: Cu(2), 0.3783 Å; Cu(3), 0.5113 Å. As in the other compounds relatively short Cu–Sb contacts are observed which are shorter than in compounds **1–3**³⁰ and **I–IV** (see above and Table 5).

The layered anion (Figure 7) contains only 6 MR: Sb(1)Cu(2)Cu(3)S₃ (6 MR A); Sb(1)Cu(1)Cu(3)S₃ (6 MR B); Sb(2)Cu(1)Cu(3)S₃ (6 MR C); Sb(2)Cu(1)Cu(2)S₃ (6 MR D); Sb(1)Sb(2)Cu(2)S₃ (6 MR E). These rings are condensed with the sequence ⋯A–B–C–D–E–A⋯ (Figure 7) forming a single layer within the (001) plane. The single layer may be viewed as an undulated distorted graphene layer with the C atoms replaced by Cu, Sb, and S atoms. Also the layer can be described as a distorted 6³ net. Two adjacent layers are joined via Cu(1)–S(4) bonds (Figure 8) yielding a double layer and Cu(2)₂S₂ rings. The double layers are stacked along [001] with the disordered amine molecules between the inorganic layers (Figure 8). The shortest interlayer separation amounts to 6.44 Å.

Spectroscopy. In the IR spectra of all compounds show bands which are typical for R–NH₃⁺ cations, and charge compensation requires that the amines are protonated.

The power of Raman spectroscopy to probe differing Sb–S bonding interactions (see Tables 2, 4, and 5) is well-known.^{41,42} The bands of the five compounds are located at 315.7 cm⁻¹ (**I**), 313.5 cm⁻¹ (**III**), 309.4 cm⁻¹ (**IV**), 315.0 cm⁻¹ (**V**) and 339.7 cm⁻¹ (**II**), 335.9 cm⁻¹ (**IV**), 336.5 cm⁻¹ (**I** and **III**), 336.6 cm⁻¹ (**V**). The resonances for the SbS₃

(41) Pflitzner, A. *Chem.—Eur. J.* **1997**, *3*, 2032–2038.(42) Pflitzner, A.; Kurowski, D. *Z. Kristallogr.* **2000**, *215*, 373–376.

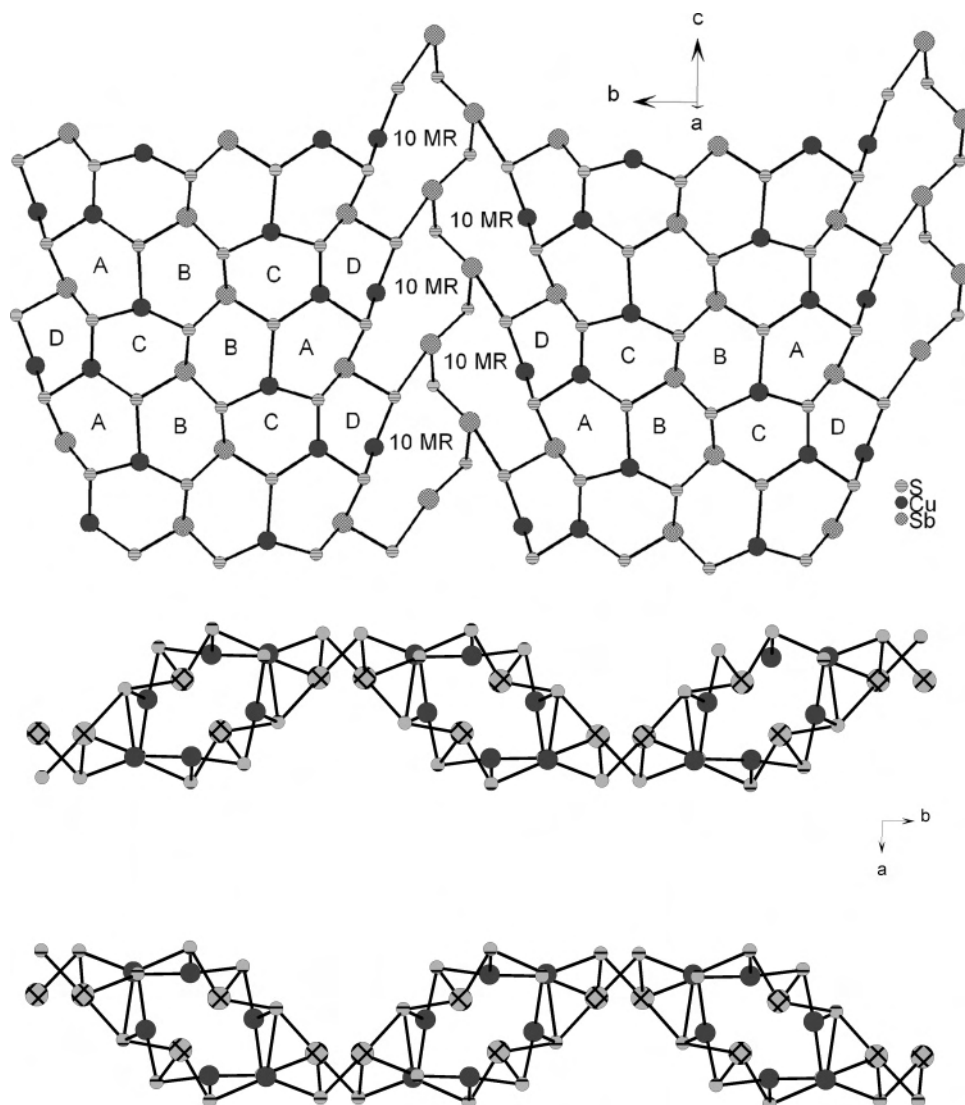


Figure 5. Condensation of the different heterorings in compound **IV** forming one layer (top). The letters identify the types of the rings (see text). View along [001] showing the packing of the undulated layers (bottom). (Note: the amine ligands which were not located are arranged between the layers.)

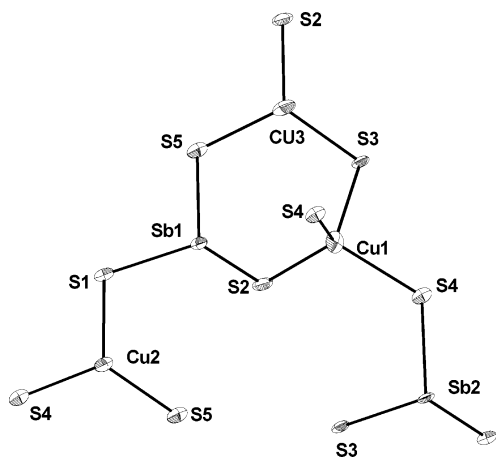


Figure 6. Crystal structure of compound **V** with labeling showing the connection of the primary building units. The displacement ellipsoids are drawn on the 50% probability level.

pyramids are observed between 362 and 339 cm^{-1} , while bands located at lower wavenumbers characterize the bonding interactions between Sb(III) and the next nearest S atoms.⁴²

Table 5. Ranges of Interatomic Distances (Å) and Angles (deg) for $(\text{C}_6\text{N}_4\text{H}_{20})_{0.5}\text{Cu}_3\text{Sb}_2\text{S}_5$ (**V**) with Estimated Standard Deviations in Parentheses

Sb(1)–S	2.406(4)–2.547(4)
Sb(1)–Cu(2)	2.869(3)
Sb(2)–S	2.398(5)–2.522(4)
Sb(2)–Cu(3)	2.683(3)
Cu(1)–S	2.340(5)–2.482(5)
Cu(2)–S	2.262(4)–2.348(4)
Cu(3)–S	2.284(4)–2.301(4)
Cu(1)–Cu(1a)	2.715(5)
S–Sb(1)–S	95.89(15)–101.45(14)
S–Sb(2)–S	93.00(15)–106.21(13)
S–Cu(1)–S	98.57(17)–119.04(18)
S–Cu(2)–S	109.77(17)–127.62(16)
S–Cu(3)–S	112.76(17)–117.39(17)

The spectra of **I–III** are similar to those reported for **1–3**.³⁰ In the three new as well as in the previously reported compounds the Sb(III) atom has 3 short and 2 significantly longer contacts to S atoms giving rise to the resonances at about 335 and 315 cm^{-1} . We note that for Cu_3SbS_3 with Sb(III) in a $3 + 5$ surrounding of S atoms the bands are observed at even lower wavenumbers, i.e., at 321 and 290

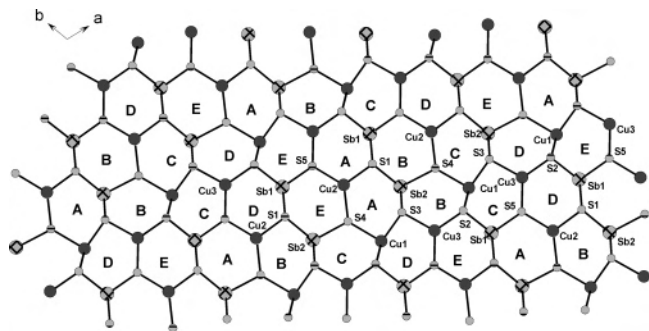


Figure 7. Crystal structure of compound **V** with labeling and view along [001] showing the sequences of the different rings.

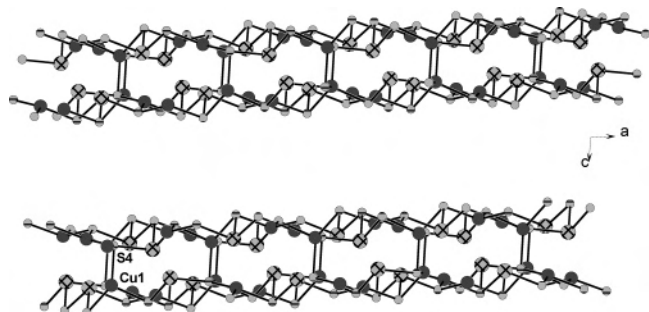


Figure 8. Crystal structure of compound **V** with view along [010] showing the interconnection of the layers into double layers via the Cu(1)–S(4) bonds.

cm^{-1} , and in MnSb_2S_4 with $3 + 2 + 1$ and $3 + 2 + 2$ environments for the two unique Sb(III) atoms the resonances are at 300 and 283 cm^{-1} .⁴²

Thermal Investigations. Compound **I** starts to decompose at $T_{\text{onset}} = 201 \text{ }^\circ\text{C}$. A weight loss of 15.9% occurs in one step being accompanied by an endothermic signal at a peak temperature $T_p = 228 \text{ }^\circ\text{C}$. The mass loss is 1% larger than expected for the removal of 1,6-diaminohexane ($-\Delta m = 14.9\%$). In the decomposition product the reflections of CuSbS_2 and Cu_3SbS_4 are identified in the X-ray powder pattern.

For compounds **II** and **III** the decomposition reactions are more complex. The two compounds seem to be less stable because decomposition starts at significantly lower temperatures. For **II** the mass starts to decrease just above $100 \text{ }^\circ\text{C}$ and the thermal decomposition reaction is accompanied by two endothermic peaks at $T_p = 204 \text{ }^\circ\text{C}$ and $T_p = 259 \text{ }^\circ\text{C}$. Compound **III** is even less stable, and the decomposition starting above about $60 \text{ }^\circ\text{C}$ proceeds over a large temperature range. The first very broad DTA peak has $T_p = 209 \text{ }^\circ\text{C}$, and the second, $T_p = 260 \text{ }^\circ\text{C}$. The total weight losses of 15.1% for **II** (calcd 14.8%) and 10.4% for **III** (calcd 11.6%) are in rough agreement with the removal of the amine molecules. In the dark gray residue of **II** about 0.5% C, H, and N were found, and for **III** the C, H, and N content in the decomposition product is 1.3% . Again, the reflections of CuSbS_2 and Cu_3SbS_4 occur in the powder patterns of the residues.

For compound **IV** the curves indicate a low stability because decomposition starts as low as about $80 \text{ }^\circ\text{C}$. Up to $450 \text{ }^\circ\text{C}$ the mass loss is 13.7% (calcd 15.1%). In the DTA curve only one pronounced signal is observed ($T_p = 185 \text{ }^\circ\text{C}$). The gray residue contains about 1.5% C, H, and N, and

only the two compounds Cu_3SbS_3 and CuSbS_2 could be identified in the powder pattern. Finally, compound **V** shows a complex thermal behavior with a beginning of decomposition at about $150 \text{ }^\circ\text{C}$. A not well-resolved endothermic event occurs at $T_p = 168 \text{ }^\circ\text{C}$, and a second one, at $T_p = 245 \text{ }^\circ\text{C}$. The total weight change of 11.5% is in rough agreement with the removal of the tetn molecules (calcd: 10.3%). Again, the gray decomposition product was contaminated with C, H, and N (2.5%) and in the X-ray powder pattern residues only reflections of Cu_3SbS_3 and CuSbS_2 were seen.

Summary

Several features of the new inorganic–organic hybrid compounds will shortly be highlighted. Compounds **I–III** are new members of the copper thioantimonate family with the general formula RCu_2SbS_3 , with R being an amine of different size and shape.^{27,30} The space between the anionic layers is determined by the size, packing, and orientation of the structure directing molecules. For the seven compounds with the layered $[\text{Cu}_2\text{SbS}_3]^-$ anion the interlayer separation reaches from 4.43 to 8.44 \AA . Applying suitable templates, it should be possible to increase the space between the anionic layers generating new inorganic–organic hybrid materials. In the structures of all compounds the orientation of the protonated amines toward the anionic layers suggests that N–H \cdots S bonds cannot be neglected.

In **I–III** as well as in compounds **1–3**³⁰ only SbS_3 and CuS_3 moieties are present, which are joined to form Cu_2SbS_3 (6 MR) and $\text{Cu}_3\text{Sb}_2\text{S}_5$ (10 MR) rings. In **IV** CuS_4 tetrahedra and SbS_4 units are present yielding a complex undulated anionic layer with 4 MR and 6 MR. The anionic layer in compound **V** is constructed by condensation of 6 MR. The tetrahedrally coordinated Cu(1) atom has one S atom in the adjacent layer yielding finally a double layer. The anions in compounds **IV** and **V** have the same chemical composition but very different structures due to the presence of different PBUs. Relatively short Cu–Cu distances are found in **IV** but only long Cu–Sb separations. In **V** the situation is opposite; i.e., short Cu–Sb distances are present but only one medium-sized Cu–Cu separation (compare Tables 4 and 5). A short Cu(2)–Cu(3) distance of $2.622(1) \text{ \AA}$ in **IV** leads to a stronger distortion of the $\text{Cu}(3)\text{S}_4$ tetrahedron compared to the $\text{Cu}(1)\text{S}_4$ tetrahedron in **V** with a longer Cu(1)–Cu(1a) separation of $2.715(5) \text{ \AA}$ (see Tables 4 and 5).

Interesting features of all compounds are short Cu–Sb separations ranging from $2.683(3) \text{ \AA}$ in **V** to about 3.1 \AA in **I–III** (compare Tables 2, 4, and 5) and the orientation of the Sb(III) $5s^2$ lone pair which always points toward the Cu(I) centers. In all cases the distances are in the range found in binary or ternary antimonides.^{43–45} Whether there are Cu–Sb bonding interactions in the title compounds cannot be decided on the basis of the interatomic separations.

(43) Nuss, J.; Jansen, M. *Z. Anorg. Allg. Chem.* **2002**, *628*, 1152–1157.

(44) Koblyuk, N. D.; Melnyk, G. A.; Romaka, L. P.; Bodak, O. I.; Fruchart, D. *J. Alloys Compd.* **2001**, *317*, 284–286.

(45) Jandali, M. Z.; Rajasekharan, T.; Schubert, K. Z. *Metallk.* **1982**, *73*, 354–359.

Calculations of the band structures are necessary to gain further insight into the bonding properties in the new copper thioantimonates.

Using the SOLV option in Platon,³⁷ the volume of the extraframework molecules in the interlayer galleries can be calculated. The values range from about 35.7% in **V** to 45.6% for **IV** (**I**, 45%; **II**, 39.4%; **III**, 37%).

As pointed out above, the anionic layered structures are constructed by condensation of Cu–Sb–S heterorings. Considering only the 6 MR, two different situations can be distinguished: Cu_2SbS_3 and CuSb_2S_3 . If only 6 MR are present, the ratio of these two different ring types determines the chemical composition of the anionic network. In **V** the ratio is 4:1 and the chemical formula is then $\text{Cu}_9\text{Sb}_6\text{S}_{15}$, which corresponds to $\text{Cu}_3\text{Sb}_2\text{S}_5$. Many more combinations of these 6 MR can be envisaged yielding other networks with a different chemical composition and new network topologies. One interesting example with Ag instead of Cu was recently published. In the $[\text{Ag}_5\text{Sb}_3\text{S}_8]^{2-}$ anion AgSb_2S_3

and Ag_2SbS_3 rings occur in a 1:7 ratio giving the overall stoichiometry of the anion.⁴⁶

The structural diversity is significantly enhanced taking also the 10 MR into account which are observed in compounds **I–III**. In the structure of **I–III** only one 6 MR type and one 10 MR type occur. Obviously, a large number of combinations of such rings are possible generating compounds with different Cu:Sb:S ratios and new network topologies. Solvothermal syntheses under different conditions are under way to further explore the Cu–Sb–S system.

Acknowledgment. The financial support by the State of Schleswig-Holstein and the Deutsche Forschungsgemeinschaft (DFG) is gratefully acknowledged.

IC050196+

(46) Vaqueiro, P.; Chippindale, A. N.; Cowley, A. R.; Powell, A. V. *Inorg. Chem.* **2003**, *42*, 7846–7851.